AdVanced Aerodynamic Tools for lArge Rotors

Choose confidentiality.

AVATAR Deliverable D1.1 Reference Blade Specification

Takis Chaviaropoulos, CRES
Henk-Jan Kooijman, GE
Jesper Madsen, LM
Gerard Schepers, ECN
Niels Sørensen, DTU
Martin Stettner, GE

March 10, 2014

Agreement n.:	FP7-ENERGY-2013-1/ n° 608396
Duration:	November 2013 to November 2017
Coordinator:	ECN Wind Energy, Petten, The Netherlands

Supported by:

Table of contents

Summary

This document represents Deliverable 1.1 of the AVATAR project, containing the specification of the AVATAR reference blade. Based on a fictive commercial scenario, a low specific power variant of the INNWIND.EU 10MW research wind turbine is specified as a replacement of the INNWIND baseline blade on this wind turbine platform.

1 Rationale

The AVATAR Description of Work defines the scope of this deliverable as "… a description of the design specifications and argumentation thereof for the AVATAR rotor", where the design "…is produced according to industry standards. As such, the design specifications, the target function and constraints are defined in consultation with industry" (Work Package 1). Subsequently, it is specified that the specification shall include aerodynamic characteristics which challenge the state-of-the-art of today's aerodynamic and aeroelastic simulation capabilities.

Blade product specifications reflect the respective wind turbine OEM's product strategy, including expected market demand, development, and competition, existing platforms and technologies, as well as risks. They are provided by the company's product management to the respective engineering teams, and contain ranges for system level parameters associated with rotor and platform. The engineering teams conduct extensive design studies and parameter sweeps within these bounds, leading, for instance, to aerodynamic candidate parameter sets. Therefore, the scope of AVATAR Deliverable D1.1 "Reference Blade Specification" is very different from industrial design specifications referred to in the description of Work Package 1; in fact D.1.1 would be the outcome, not the starting point of an industrial type specification.

This section provides a link between these two very different types of specifications by first indicating a fictive commercial scenario (mimicking the scope of the information provided by product management to engineering). In lieu of the initial step in parametric design studies, system level considerations are presented next. Finally, a scaling methodology basing on first principles is presented and applied to derive key aerodynamic specifications. The bulk part of this document contains a few key aerodynamic parameters and constraints.

Throughout this document, the "baseline 10MW wind turbine" referred to is the INNWIND.EU research wind turbine / DTU 10MW RWT (Bak, et al.). AVATAR modifications to this configuration are explained in this document's text. All data not explicitly referred to in this text as modifications are taken without change from this data set.

1.1 Fictive Commercial Scenario

In the presented scenario, a market for medium to deep water offshore wind energy has been identified in the 40-50 m water depth range. IEC class 1A is representative of typical wind conditions. Offshore areas assigned for wind park development permit installation of large, regular grid type arrangement of individual wind turbines.

Cost of Energy, CoE, has been identified as the key metric of competitiveness. As distance to shore is significant, substantial investments into substructures and grid connection with onshore connectors are required, so significant increases in energy production and/or investment cost reductions are necessary compared to the state-of-the-art of offshore wind turbines.

Near shore manufacturing potential for key components is weak, but component manufacturers are within range for economic land transport. Significant cost increases incur when dimensions of shipped components exceed an equivalent 60m×3.5m×3.5m box.

A 10MW offshore demonstrator (Bak, et al.) is technically suitable for the identified market and was selected as platform for the target market. This includes the existing jacket-type substructure. Commercial considerations based on proven practice for reduction of onshore CoE suggest development of a significantly more cost-effective, high capacity factor, low specific power variant of this demonstrator. In the offshore context, benefits are expected both from higher predictive output, i.e. more full load hours, and more effective use of energy transport cables (MWh/MW). An optimal specific power of 300 W/m² (75% of the baseline wind turbine's value) is projected, requiring a substantially larger rotor. To exploit in-service experience gathered with this platform and minimize re-design cost, changes to all baseline components including the substructure are to be avoided wherever possible.

Following a trend in the industry, the new product shall include control and communication features enabling the individual wind turbines as elements of the overall wind park context, permitting close spacing and increased park output. As a result, the new rotor is to be designed for frequent exposure to wakes of upwind machines, and extended period power production in yaw in order to exploit wake steering.

1.2 System Level Considerations and Scaling

The fictive scenario above is now used to derive main parameters of the low specific power wind turbine, and provide the base for a blade design specification. Key parameters of the baseline 10MW platform are 401 W/m² specific power and 9.6rpm nominal rotor speed, the rotor diameter is 178.4m, rated wind speed is 11.4 m/s, hub height is 119m (Bak, et al.)

First principles adapted from GL Guidelines, and rotor weight as a given function of diameter are used to generate a scaled version to help understand the main limiting factors if one progresses along today's technology trend lines, specifically blade static moment, and normal power production thrust loading. When rated power and nominal rotor speed are kept unchanged as specified, using the ratio of specific powers, $\bar{s}$, as scaling factor, leads the scaling rules shown in the second column of Table 1.

In plane aerodynamic blade moments and main shaft torque at nominal power are unchanged. Results for $\bar{s}$ = 75% are summarized in Table 2 (second column), showing clearly that loads for the up-scaled, 205.76m diameter rotor exceed the baseline values significantly. The 10% increase in thrust is particularly costly: Observing a relaxed 25m clearance between blade tip and mean sea level, MSL[1], the new wind turbine's hub height grows by 8% to 127.9m, resulting in a 18% increase in support structure base overturning moment. This requires strengthening of both tower and substructure, leading to significant cost increases. Significant rotor design changes due to up-scaling are imperative, alternative design solutions must be explored.

For the same rotor diameter, thrust at rated wind speed can be reduced by selecting a lower induction and reduced power coefficient, requiring higher design rated speed to recover name plate power (Table 2, third column). Low induction is favorable both in terms of load reduction and in terms of wind farm aspects: Wake losses and wake induced turbulence levels near nominal power are reduced, which permits revisiting the trade-off between wind turbine spacing and energy capture.

Scaling the induction ratio is straightforward in implementation, but scaling design (rated) wind speed provides more insight into the impact on energy capture. Hence, the ratio of design rated speeds, $\bar{v}$, is added as second, independent scaling parameter.

Exploiting momentum theory to obtain induction changes the scaling of power coefficient, induction, thrust coefficient, and aerodynamic bending moments: The ratio of inductions, $\bar{a}$, can be obtained from the ratio of power coefficients, $\bar{C}_P = \bar{s}\bar{v}^{-3}$, and the induction of the reference rotor, a_{ref}, by solving

$$\bar{a}\frac{(1-\bar{a}a_{ref})^2}{(1-a_{ref})^2} - \bar{C}_P = 0 \quad (1)$$

The respective solution is (see Appendix A)

$$\bar{a} = \frac{1}{3a_{ref}}\left(2-\sqrt{3}\cos\left(\frac{\psi}{3}\right)+\sin\left(\frac{\psi}{3}\right)\right);\ \psi = \sin^{-1}(u);\ u = \frac{27}{2}(a_{ref}-1)^2 a_{ref}\,\bar{C}_P - 1 \quad (2)$$

[1] The baseline rotor uses about 30m

Table 1 (third column) contains the respective scaling rules, using short hand notation for power and thrust coefficient ratios, $\bar{C}_P$ and $\bar{C}_T$, to maintain a compact representation at the expense of transparency of dependency on $\bar{s}$ and $\bar{v}$. Fitting the exact solutions for $\bar{a}$ and $\bar{C}_T$ with exponential function to base $\bar{C}_P$ eliminates the short hand notation, but provides little more insight into the trends (Table 1, fourth column; with the given coefficients, the error in induction ratio, $\bar{a}$, and thrust coefficient ratio, $\bar{C}_T$, are 0.8% and 0.42%, respectively).

Scaling $\boldsymbol{coefficients\ for\ a_{\mathrm{ref}} = 0.3\ (see\ Appendix\ A)}$: $\boldsymbol{k_1 = 0.496;\ k_2 = 0.490; k_3 = 7.389;}$ $\boldsymbol{k_4 = 0.551;\ k_5 = 0.444; k_6 = 5.557;}$	**Specific power**	**Specific power & rated wind speed**	**Specific power & rated wind speed (approximation)**
Rotor Diameter	$\bar{s}^{-1/2}$	$\bar{s}^{-1/2}$	$\bar{s}^{-1/2}$
Rated Wind Speed	$\bar{s}^{1/3}$	$\bar{v}$	$\bar{v}$
Power coefficient	1	$\bar{s}\bar{v}^{-3} := \bar{C}_P$	$\bar{s}\bar{v}^{-3}$
Induction	1	$\bar{a}(a_{\mathrm{ref}}, \bar{C}_P)$, eq. (2)	$k_1 + k_2(\bar{s}\bar{v}^{-3})^{k_3}$
Thrust coefficient	1	$\bar{a}\dfrac{1-\bar{a}a_{\mathrm{ref}}}{1-a_{\mathrm{ref}}} := \bar{C}_T$	$k_4 + k_5(\bar{s}\bar{v}^{-3})^{k_6}$
Axial thrust	$\bar{s}^{-1/3}$	$\bar{s}^{-1}\bar{v}^2\bar{C}_T$	$k_4\bar{s}^{-1}\bar{v}^2 + k_5\bar{s}^{(k_6-1)}\bar{v}^{(2-3k_6)}$
Blade moments, aerodynamic, out of plane	$\bar{s}^{-5/6}$	$\bar{s}^{-3/2}\bar{v}^2\bar{C}_T$	$k_4\bar{s}^{-3/2}\bar{v}^2 + k_5\bar{s}^{(k_6-3/2)}\bar{v}^{(2-3k_6)}$
Main shaft bending moment	$\bar{s}^{-5/6}$	$\bar{s}^{-5/6}$	$\bar{s}^{-5/6}$
Blade moments, E-stop[2], in plane	$\bar{s}^{-7/4}$	$\bar{s}^{-7/4}$	$\bar{s}^{-7/4}$
Blade moments, inertial[3], out of plane	$\bar{s}^{-9/4}$	$\bar{s}^{-9/4}$	$\bar{s}^{-9/4}$

Table 1: Scaling rules

[2] The brake situation is here assumed to be governed by a short circuit event for which the torque is typically proportional to the nominal torque, proportional to diameter$^{3.5}$

[3] Inertia load is proportional to (blade mass) × (cog offset)^2, i.e. diameter$^{2.5}$ × diameter^2 = diameter$^{4.5}$.

Applying these rules for $\bar{v}$ = 92.5% (rated wind speed 10.55 m/s) and assuming a baseline rotor induction a_{ref} = 0.30 results in a rotor producing the same thrust at rated speed as the baseline rotor (Table 2, third column). The respective induction is reduced from 0.30 to 0.24, the power coefficient from 0.44 (as derived from specific power and rated wind speed) to 0.42. As shown above, observation of MSL clearance results in an 8% growth in hub height, leading to an 8% increase in support structure overturning moment. Blade root bending moments from aerodynamic loads increase by 15% (Table 2, third column).

Evidently, scaled rotor growth leads to inertial loading increases in excess of 65% (edgewise) and 95% (flapwise) which is unacceptable within the blade retrofit scenario. Mitigation is possible by breaking with the $R^{2.5}$ mass growth implicit to the scaling rules presented on the previous page. The AVATAR reference blade may therefore employ high cost carbon composites, enabling a lower mass design.

Scaling by	$\bar{s}$ **= 75%**	$\bar{s}$ **= 75%** $\bar{v}$ **= 92.5%**
Rotor diameter	+15%	+15%
Rated wind speed	-9%	-7.5
Induction	0%	-19%
Axial thrust	+10%	0%
Support structure overturning moment	+18%	+8%
Blade moments, aerodynamic, out of plane	+27%	+15%
Main shaft bending moment	+27%	+15%
Blade moments, E-stop, in plane	+65%	+65%
Blade moments, inertial, out of plane	+91%	+91%

Table 2: Changes for scaled variants, compared to baseline INNWIND.EU

1.3 Aerodynamic Specification and R&D Perspective

The AVATAR rotor will operate at uncommon conditions, even compared to the INNWIND baseline, and challenge the validity of existing design and analysis tools. In terms of the design process, particular attention is needed in the context of the following:

- more spatial variation in flow conditions due to the large rotor diameter, and different unusual induction require CFD studies to tune and enhance engineering codes;
- high Reynolds numbers require wind tunnel testing to assess the validity of aerodynamic predictions;
- higher tip speeds necessitate in-depth aeroelastic analysis to avoid instabilities;
- tight component load limits in conjunction with performance requirements may dictate addition of active devices; function and objective of such devices must be clearly defined (increase c_P, reduce storm loading, better secure attached flow, etc.)

2 Operation

2.1 Rotor Design Point

The AVATAR rotor shall be operated at the same design rotational speed as the INNWIND rotor (9.6 rpm) and wind speed range (cut-in at 4 m/s, cut-out at 25 m/s). From the scaling procedure above, a design rated speed of 10.5 m/s, tip speed of 103.4 m/s and tip speed ratio of 9.8 are projected; these values need to be confirmed by detailed analysis and/or adjusted to meet performance targets and load limits.

2.2 Wind

The AVATAR rotor shall be designed for wind class IA according to IEC61400-1 Ed. 3 standard (IEC, 2005), with wind speed distribution during life time identical to that used for the INNWIND rotor ((Bak, et al.) p. 74 Table 6.8), and using the Mann turbulence model.

2.3 Design Load Cases

The INNWIND rotor design excluded controller-related design load cases (DLC1.4, DLC2.2, DLC3.1, DLC3.2, DLC3.3; chapter 6.3 of INNWIND (Bak, et al.)); AVATAR rotor design shall follow the same philosophy, but aeroelastic analysis (evaluation Tasks 1.3 and 1.6 of the AVATAR DoW) of the final designs for AVATAR “baseline” and AVATAR “improved” shall include the full set of design load cases.

3 Wind Turbine System

The top level specification requires the AVATAR wind turbine system – except the rotor – to be largely identical to the INNWIND platform. In the following section, only key values of this data set are repeated where required as reference for modifications in AVATAR.

3.1 Rotor

The AVATAR and INNWIND.EU concept are identical. The precone angle of -2.5° may have to be adjusted to meet prebend and tower clearance limitations concurrently. The rotor diameter is 205.76m.

3.2 Pitch Actuation

The AVATAR and INNWIND.EU concept are identical. 2°/sec and 5°/sec will be considered as pitch velocity for normal and emergency shut-down case ((Bak, et al.), section 6.3), maximum pitch velocity in operation in 10°/sec ((Bak, et al.) chapter 5). A pitch system re-design to address changes to the control system (section 3.7) is considered out of scope in AVATAR; however, the impact on system cost and dynamics shall be addressed in the evaluation tasks.

3.3 Nacelle and Hub

The AVATAR and INNWIND.EU concepts are identical. As no details on bedplate flexibility are given in (Bak, et al.), this component is considered as rigid. Refer to (Bak, et al.), Tables 2.1 and 6.1 for details.

3.4 Shaft, Drivetrain, and Generator

The AVATAR and INNWIND.EU concepts are identical. The INNWIND gear box is of medium speed design with gear box ratio of 50:1, generator type and torque-speed characteristics are unspecified. Refer to (Bak, et al.), Tables 2.1, 6.2, and 6.3 for details.

3.5 Tower

(1) Re-design of the tower is out of scope within the AVATAR program. The tower shall therefore remain unchanged in height. Tower top and bottom diameter shall be maintained to ensure compatibility with yaw drive and substructure connector. The impact of strengthening the tower, if required, on system cost and dynamics shall be addressed by simple scaling rules. Addressing the blade tip-MSL clearance constraint in a system cost context is left for future investigation.

(2) The AVATAR wind turbine rotor will grow compared to the INNWIND value at the same rate as blade length, resulting in a 15% increase to 137.5m. Tower top and bottom diameter shall be maintained to ensure compatibility with yaw drive and substructure connector. The impact of strengthening the tower, if required, on system cost and dynamics shall be addressed by simple scaling rules.

3.6 Sub Structure

The AVATAR and INNWIND.EU concepts are identical (jacket type). As no details on substructure flexibility and damping are given in (Bak, et al.); should no additional information become available from the INNWIND program before launch of Task 1.2 "Reference Blade Design" (via AVATAR Task 1.7), then the foundation will be considered rigid.

3.7 Control System

The INNWIND wind turbine uses PI feedback laws to control collective blade pitch and generator torque. The AVATAR system shall also include individual pitch control to reduce cyclic loading, which is considered current industrial state-of-the-art and essential to maintain acceptable rotor load levels.

4 Blade Design Process, Integrity, and Material Properties

The AVATAR blade shall be designed for a cost of energy related objective function comprised of energy production, blade mass breakdown, and key component loads, observing constraints set forth in the following sections. A thorough performance vs. component cost trade-off would require a concurrent aerodynamic-structural-control-loads design process. For the AVATAR needs a simplified sequential design approach may be followed for the reference blade design where justification for the design choices will be provided, starting with the detailed aerodynamic layout (which is mostly important for the AVATAR needs), followed by structural layout (for minimized use of material), and loads/controls design. Design variables as described in the following shall be permitted to impact the objective function directly; justification shall be provided where sub-level, disciplinary optimization with a limited set of design variables is performed. The sensitivity of the final design choice to modified weighting in the objective function, constraint settings and design variables shall be assessed.

Aerodynamic design shall include freedom in the choice of induction in addition to planform design variables. Scaling as described in section 1.2 suggests an initial value of 0.24 for the induction and 0.44 for the power coefficient. Placement of seed airfoils shall be limited by geometric constraints representing simplified consideration of manufacturing constraints. Provisions for segmentation shall be included where an impact on blade shape is expected, for instance by lower bounds on blade thickness in the vicinity of blade joints. Noise shall be addressed within the evaluation Tasks 1.3 and 1.6 but noise analysis within the design loop, and consideration of noise constraints is not required. Suitability of the blade shape to installation of flow control devices like flaps, slats, or vortex generators shall be addressed.

Structural design shall follow a similar approach to INNWIND except for the material choice. Carbon fibers may be used for the spar cap to facilitate meeting tip clearance constraints while maintaining reasonable blade root bending moments from mass loads, compared to the INNWIND baseline. For the purpose of finding an optimum blade design, limitation of the design space to spar cap and leading and trailing edge thickness/cross-section, considering laminate strain limits only, is acceptable. The final design shall be checked using 3D FEM analysis to address buckling.

Adjusting controller parameters shall be addressed as part of the evaluation Tasks 1.3 and 1.6 to permit load reduction in operation (see also sections 2.3 and 3.7). The impact of non-operational events shall be addressed. Blade design shall consider constraints on a few key component loads to facilitate integration into the baseline wind turbine, see the following chapter.

5 Blade – System Integration

Based on the retrofit scenario sketched in section 1.1, modifications to INNWIND wind turbine system components shall be avoided. Scaling considerations in section 1.2 revealed that some load increases cannot be avoided though. Table 3 provides an overview of acceptable loads, based on scaling considerations outlined in section 1.2.

Details on the blade-hub interface are unavailable and detailed structural (re-) design is considered out-of-scope in AVATAR. Hence, root design is excluded; structural properties of the root shall be estimated based on the INNWIND design and scaling considerations.

In accordance with (Bak, et al.) section 6.4.5, blade tip clearance in operation shall be larger than 30% of the static value, and 5% in parked conditions. Coalescence of system eigenvalues with 3 times and 6 times the rotor speed shall be avoided with a 15% margin.

Load	**Value/Target (diff to base)**	**Min**	**Max**	**Section; Reference (in (Bak, et al.))**
Axial thrust	4620kN (+0%)			1.2; 4.2.4
Tower top bending Moment, extreme			21,028 kNm (+15%)	1.2; 4.2.4
Tower bottom bending moment resultant, extreme			74,466 kNm (+8%)	1.2; Figure 6.3
Tower bottom fore-aft bending moment, fatigue DEL			47,520 kNm (+8%)	1.2; Figure 6.7

Table 3: AVATAR load limits, compared to INNWIND baseline

6 Cross Section

6.1 Airfoil Families

The AVATAR reference blade shall utilize airfoils of the DU family. This choice is based on considerations related to the AVATAR objective of providing validated methods for challenging aerodynamic conditions:

- DU airfoil data are publically available.

- A reasonably large data base of experimental and numerical results exists.

In addition, choosing airfoils different from those employed in INNWIND adds value since the challenges in modeling transition will be addressed for two separate airfoil families.

Applicability of the aerodynamic characteristics of these airfoils in the operating range of the AVATAR rotor shall be addressed; this includes in particular Mach numbers up to 0.3 and Reynolds numbers up to 18 million in the tip region. Lower bounds on trailing edge thickness shall be the maximum of 1% of chord or 3mm.

6.2 Structural Concept

The AVATAR rotor blade shall use a two-spar cross section largely following the INNWIND concept in layout and material choice, and utilize INNWIND progress as available at the time of launch of Task 1.4 “Reference Blade Design” activities. Exceptions to the current INNWIND concept are

- The spar cap width shall be constant along the blade span, unless limited by blade chord.
- A third shear web in the tip regions is to be avoided. Justification shall be provided if the added complexity and cost cannot be avoided.
- The skin’s tri-axial laminate shall not be interrupted by the spar cap, but continue all around the cross-section. Carbon fiber based laminates are acceptable for the spar cap to facilitate meeting blade inertia and deflection related constraints.

The thicknesses of unidirectional laminates in spar cap, as well as leading edge and trailing edge re-enforcements shall be considered as design freedom. Skin, shear web, and blade root design shall be based on the INNWIND concept. Non-structural mass from lightening protection, chordwise segmentation, blade joints etc. shall be included; an estimation of these masses is sufficient. Provisions for segmentation shall be included where an impact on blade shape is expected, for instance by lower bounds on blade thickness in the vicinity of blade joints – a structural analysis of blade joints is not required. Modification of structural twist and bend-twist coupling using tailored laminates shall not be considered.

7 Reference Line

Blade prebend shall be based on the INNWIND rotor’s curve (blade deflection curve at operation in 5 m/s wind speeds ((Bak, et al.), section 3.4, p. 25)), scaled geometrically to account for the AVATAR rotor’s larger diameter. Increasing prebend to meet tower clearance constraints is permitted, but prebend shall not be altered unless tower clearance constraints are violated Sweeping the blade reference line shall be considered to exploit (geometric) bend-twist coupling for load reduction. A low order function shall be employed to limit the design space to smooth reference lines. Maximum prebend and presweep could be limited to avoid transportation issues (section 1.1).

8 Thickness, Twist and Planform

In the following limits of the parameters describing the blade geometry are defined. Although thorough in-depth analysis of the geometric relations for both manufacturability and structural complexity are not presently available, the limits are supported by industry experience. The limits are divided up into two parts; the first part concerns absolute values and the second part concerns the smoothness of the geometry parameters.

8.1 Absolute Values

The constraints on absolute values are:

- The maximum allowed chord length is 7.13 m. This value is linearly scaled up from the 6.2 m maximum chord length on the INNWIND blade.
- The maximum absolute thickness of the root region up to 10m or radius shall be limited to the INNWIND value of 5.38 m. This thickness is quite small for the root and may have to be increased slightly.
- The minimum blade tip chord and thickness at a distance of 350 mm from the tip shall be limited to 300 mm and 60 mm, respectively. This will allow for room for lightning protection systems.
- The difference between maximum and minimum twist of the blade shall not exceed 18°.

8.2 Smoothness of Geometry Parameters

Before a smooth 3D blade geometry can be obtained, the main geometry parameters must be adjusted in value to ensure smooth distributions.

The main geometry parameters are:

- Chord
- Relative Thickness
- Absolute Thickness
- Twist
- Prebend
- Normalized distance from the leading edge to the pitch axis

The purpose of the geometry parameter smoothness limits is to avoid waviness in the blade geometry which is unwanted due to manufacturability or structural considerations. The blade will have natural waves in the geometry parameters, e.g. the bump on the chord distribution around the maximum chord area. The task is to filter away the unwanted waves, which serves no purpose.

To limit the waves in geometry parameters, the mapping of the parameters with their first and second order derivatives with the z-axis as reference should be used. These facilitate the detection and the measuring of waves in the geometry parameters. The first derivative represents the slope of the parameter. The first derivative will not detect waves, as well as the second derivative, but it will help understand the shape of the waves. The second derivative represents the curvature of the parameter, and by analyzing the second derivative waves will be detected.

In order to be general for different blades, z-position (along pitch axis), chord, and absolute thickness are normalized as follows:

Relative z-position: $RelZ = \frac{z - L_{Cylinder}}{L - L_{Cylinder}}$

Relative Chord: $RelChord = \frac{Chord}{L}$

Relative Absolute Thickness: $RelThick = \frac{Absolute\text{ Thickness}}{L}$

where $L_{Cylinder}$ is the length of the blade root cylinder and L is the blade length.

Minimum and maximum values for derivatives of *RelChord*, *ThickPct*, *RelThick*, and *Twist* with *RelZ* as the reference are given in Table 4, Table 5, Table 6, and Table 7, respectively. For positions in between positions given in the tables, the limits should be interpolated linearly.

Figure 3, Figure 4, Figure 5, and Figure 6 in Appendix B show the main geometry parameter distributions for the INNWIND blade together with the AVATAR blade minimum and maximum values for the derivatives. As can be seen most of the INNWIND blade parameters have first and second derivatives within the AVATAR blade limits. The *Twist* goes slightly beyond the limit on both first order and second order derivative. The *RelThick* distribution requirements are the most critical, and it is also seen that the INNWIND blade exceeds the AVATAR blade limits. It means that the AVATAR blade has to reduce less rapidly in absolute thickness. This can be obtained by increasing relative thickness, which puts further challenges to the aerodynamics.

Limits are not given for the prebend and distance to LE distributions; however, some overall requirements to the distributions are described in Section 7. Both distributions have to be smooth but can be adjusted to meet other requirements.

Derivative	$\frac{\partial RelChord}{\partial RelZ}$ [-]		$\frac{\partial^2 RelChord}{\partial RelZ^2}$ [-]	
RelZ	Min	Max	Min	Max
0.0	0.00E+00	1.61E-01	-2.54E+00	2.54E+00
0.1	0.00E+00	1.61E-01	-2.54E+00	2.54E+00
0.2	-1.61E-01	1.61E-01	-2.54E+00	5.33E-01
0.4	-1.61E-01	0.00E+00	-5.33E-01	5.33E-01
0.8	-1.61E-01	0.00E+00	-5.33E-01	5.33E-01
0.9	-1.61E-01	0.00E+00	-1.33E+00	5.33E-01
1.0	-2.21E+00	0.00E+00	-9.65E+01	0.00E+00

Table 4: Chord distribution requirements.

Derivative	$\frac{\partial ThickPct}{\partial RelZ}$ [%]		$\frac{\partial^2 ThickPct}{\partial RelZ^2}$ [%]	
RelZ	Min	Max	Min	Max
0.0	-6.07E+02	0.00E+00	-1.85E+05	7.55E+03
0.1	-6.07E+02	0.00E+00	-1.86E+03	7.55E+03
0.2	-2.41E+02	0.00E+00	-6.08E+02	2.47E+03
0.4	-7.27E+01	0.00E+00	-6.08E+02	6.08E+02
0.8	-7.27E+01	0.00E+00	-6.08E+02	6.08E+02
0.9	-7.27E+01	0.00E+00	-6.08E+02	6.08E+02
1.0	-1.20E+02	0.00E+00	-4.05E+04	1.34E+04

Table 5: Relative thickness distribution requirements.

Derivative	$\frac{\partial RelThick}{\partial RelZ}$ [-]		$\frac{\partial^2 RelThick}{\partial RelZ^2}$ [-]	
RelZ	Min	Max	Min	Max
0.0	-5.60E-02	0.00E+00	-4.24E+01	0.00E+00
0.1	-1.27E-01	0.00E+00	-1.18E+00	0.00E+00
0.2	-1.27E-01	0.00E+00	0.00E+00	7.38E-01
0.4	-5.27E-02	0.00E+00	0.00E+00	4.43E-01
0.8	-2.64E-02	0.00E+00	-6.40E-02	6.40E-02
0.9	-2.64E-02	0.00E+00	-1.50E-01	0.00E+00
1.0	-2.89E-01	0.00E+00	-1.06E+01	0.00E+00

Table 6: Absolute thickness distribution requirements.

Derivative	$\frac{\partial Twist}{\partial RelZ}$ [°]		$\frac{\partial^2 Twist}{\partial RelZ^2}$ [°]	
RelZ	Min	Max	Min	Max
0.0	-4.73E-01	4.73E-01	-4.69E+02	4.69E+02
0.1	-4.79E+01	4.79E+01	-4.69E+02	4.69E+02
0.2	-4.79E+01	4.79E+01	-9.23E+02	9.23E+02
0.4	-3.42E+01	3.42E+01	-1.66E+02	1.66E+02
0.8	-1.71E+01	1.71E+01	-1.66E+02	1.66E+02
0.9	-4.02E+01	4.02E+01	-5.50E+02	5.50E+02
1.0	-6.82E+02	6.82E+02	-6.18E+03	6.18E+03

Table 7: Twist distribution requirements.

References and Applicable Guidelines

Bak, C., Zahle, F., Bitsche, R., Kim, T., Yde, A., Henriksen, L., et al. (kein Datum). Design and performance of a 10 MW wind turbine (to be accepted). *J. Wind Energy*.

IEC. (August 2005). IEC 61400-1: Wind Turbines - Part 1: Design Requirements. Standard. *Standard*.

Appendix A: Scaling Rule Derivations

Ratio of Inductions

From simple momentum theory, the ratio of power coefficients is

$$\bar{a}\frac{(1-\bar{a}a_{\mathrm{ref}})^2}{(1-a_{\mathrm{ref}})^2} - \bar{C}_P = 0 \qquad \text{(i)}$$

Using the short hand notations

$$u = \frac{27}{2}(a_{\mathrm{ref}}-1)^2 a_{\mathrm{ref}}\bar{C}_P - 1 \qquad \text{(ii)}$$

and

$$v = \sqrt[3]{u + i\sqrt{1-u^2}} \qquad \text{(iii)}$$

the general solution of equation (i) for $\bar{a}$ is

$$\bar{a} = \frac{1}{3a_{\mathrm{ref}}}\begin{cases} 2 + \frac{1}{v} + v \\ 2 - \frac{1+i\sqrt{3}}{2}\frac{1}{v} - \frac{(1-i\sqrt{3})}{2}v \\ 2 - \frac{1-i\sqrt{3}}{2}\frac{1}{v} - \frac{(1+i\sqrt{3})}{2}v \end{cases} \qquad \text{(iv)}$$

Expressing v as

$$v = x + \mathrm{i}y \qquad \text{(v)}$$

yields

$$\bar{a} = \frac{1}{3a_{\mathrm{ref}}}\begin{cases} 2 + x\,\frac{x^2+y^2+1}{x^2+y^2} + iy\frac{x^2+y^2-1}{x^2+y^2} \\ 2 - \frac{x+\sqrt{3}y}{2}\,\frac{x^2+y^2+1}{x^2+y^2} + i\,\frac{\sqrt{3}x-y}{2}\,\frac{x^2+y^2-1}{x^2+y^2} \\ 2 - \frac{x-\sqrt{3}y}{2}\,\frac{x^2+y^2+1}{x^2+y^2} - i\,\frac{\sqrt{3}x+y}{2}\,\frac{x^2+y^2-1}{x^2+y^2} \end{cases} \qquad \text{(vi)}$$

Noting that

$$v = \sqrt[3]{re^{i\varphi}} \text{ with } r = \sqrt{u^2 + (\sqrt{1-u^2})^2} = 1 \qquad \text{(vii)}$$

such that

$$|v| = \sqrt[3]{r} = \sqrt[3]{\sqrt{u^2 + (\sqrt{1-u^2})^2}} = \sqrt{x^2 + y^2} = 1 \quad \Rightarrow \quad \frac{x^2+y^2+1}{x^2+y^2} = 2; \ \frac{x^2+y^2-1}{x^2+y^2} = 0 \qquad \text{(viii)}$$

results in simplification of (vi) by elimination of the imaginary part of each solution:

$$\bar{a} = \frac{2}{3a_{\text{ref}}} \begin{cases} 1 + x \\ 1 - \frac{x+\sqrt{3}y}{2} \\ 1 - \frac{x-\sqrt{3}y}{2} \end{cases} \qquad \text{(ix)}$$

The (real) unknowns, x and y, can be determined from the general expression for the cubic root of a complex number, and exploiting the fact that the absolute value of v is unity,

$$v = \sqrt[3]{re^{i\varphi}} = \begin{cases} e^{i(\varphi/3)} \\ e^{i(\varphi/3+2/3\pi)} \\ e^{i(\varphi/3-2/3\pi)} \end{cases}; \varphi = tan^{-1}\left(\frac{\sqrt{1-u^2}}{u}\right) \qquad \text{(vii)}$$

and collecting real and complex parts:

$$(x,y) = \begin{cases} (2\cos(\frac{\varphi}{3}), 2\sin(\frac{\varphi}{3})) \\ (-\frac{1}{2}(\cos(\frac{\varphi}{3}) + \sqrt{3}\sin(\frac{\varphi}{3})), -\frac{1}{2}(\sin(\frac{\varphi}{3}) - \sqrt{3}\cos(\frac{\varphi}{3}))) \\ (-\frac{1}{2}(\cos(\frac{\varphi}{3}) - \sqrt{3}\sin(\frac{\varphi}{3})), -\frac{1}{2}(\sin(\frac{\varphi}{3}) + \sqrt{3}\cos(\frac{\varphi}{3}))) \end{cases} \qquad \text{(xi)}$$

Inserting (xi) into (ix), defining

$$\psi = \sin^{-1}(u) \qquad \text{(xii)}$$

and identifying the smallest root finally results in

$$\bar{a} = \frac{1}{3a_{\text{ref}}}(2 - \sqrt{3}\cos(\tfrac{\psi}{3}) + \sin(\tfrac{\psi}{3})) \qquad \text{(xiii)}$$

In order to return to an exponential form more suitable for scaling, the following curve fit is obtained:

$$\bar{a} \approx k_1 + k_2 \bar{C}_P^{\,k_3}; \begin{cases} k_1 = 0.24 + 2.65a_{\text{ref}} - 5.99{a_{\text{ref}}}^2 \\ k_2 = 0.49 \\ k_3 = 26.13a_{\text{ref}} \end{cases} \tag{xiv}$$

This fit produces an error bound by (-2%, +4%) with the largest error for scaling near the ideal reference rotor, as depicted in Figure 1. This fit is good for transparency, but should not be used for scaling.

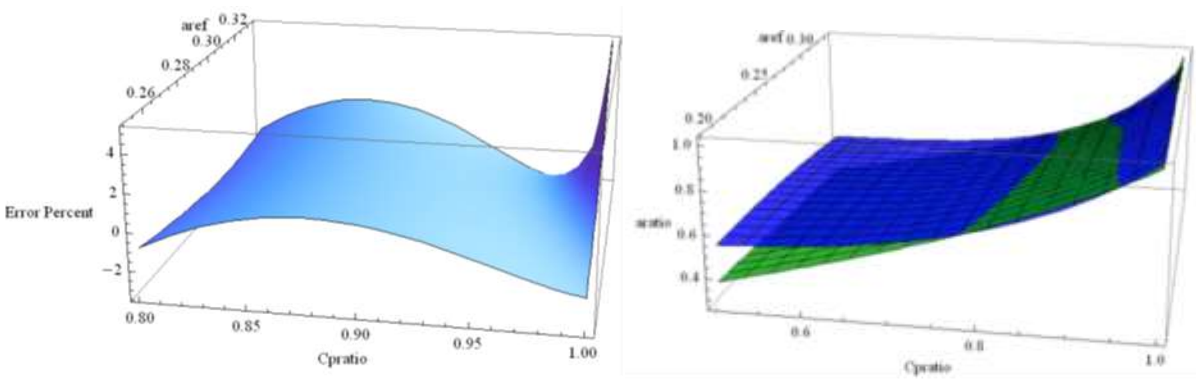

Figure 1: Fit for ratio of inductions; error (left), and exact expression [green] vs. fit [blue] (right)

Ratio of Thrust Coefficients

Inserting (xiii) into

$$\bar{C}_T = \bar{a}\frac{1-\bar{a}a_{\mathrm{ref}}}{1-a_{\mathrm{ref}}} = \frac{1-a_{\mathrm{ref}}}{1-\bar{a}a_{\mathrm{ref}}}\bar{C}_P \qquad \text{(xv)}$$

yields

$$\bar{C}_T = \frac{3(1-a_{\mathrm{ref}})}{1+\sqrt{3}\cos(\frac{\psi}{3})-\sin(\frac{\psi}{3})}\bar{C}_P \qquad \text{(xvi)}$$

The following exponential fit may be used for scaling and for depicting trends,

$$\bar{C}_T \approx k_4 + k_5\bar{C}_P^{\;k_6}\begin{cases} k_4 = 0.50 + 0.17a_{\mathrm{ref}} \\ k_5 = 0.57 - 0.42a_{\mathrm{ref}} \\ k_6 = 1 + 0.19a_{\mathrm{ref}} + 50{a_{\mathrm{ref}}}^2 \end{cases} \qquad \text{(xvii)}$$

with an error bound by (-2.5%, 1%), Figure 2.

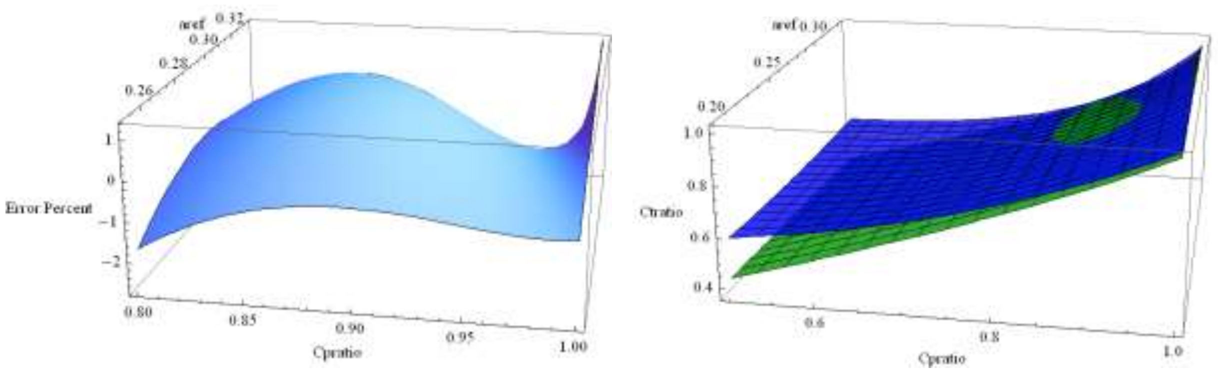

Figure 2: Fit for ratio of thrust coefficients; error (left), and exact expression [green] vs. fit [blue] (right)

Appendix B: Blade Geometry Parameter Distributions

Figure 3, Figure 4, Figure 5, and Figure 6 show the main geometry parameter distributions for the INNWIND blade together with the AVATAR blade minimum and maximum values for the derivatives.

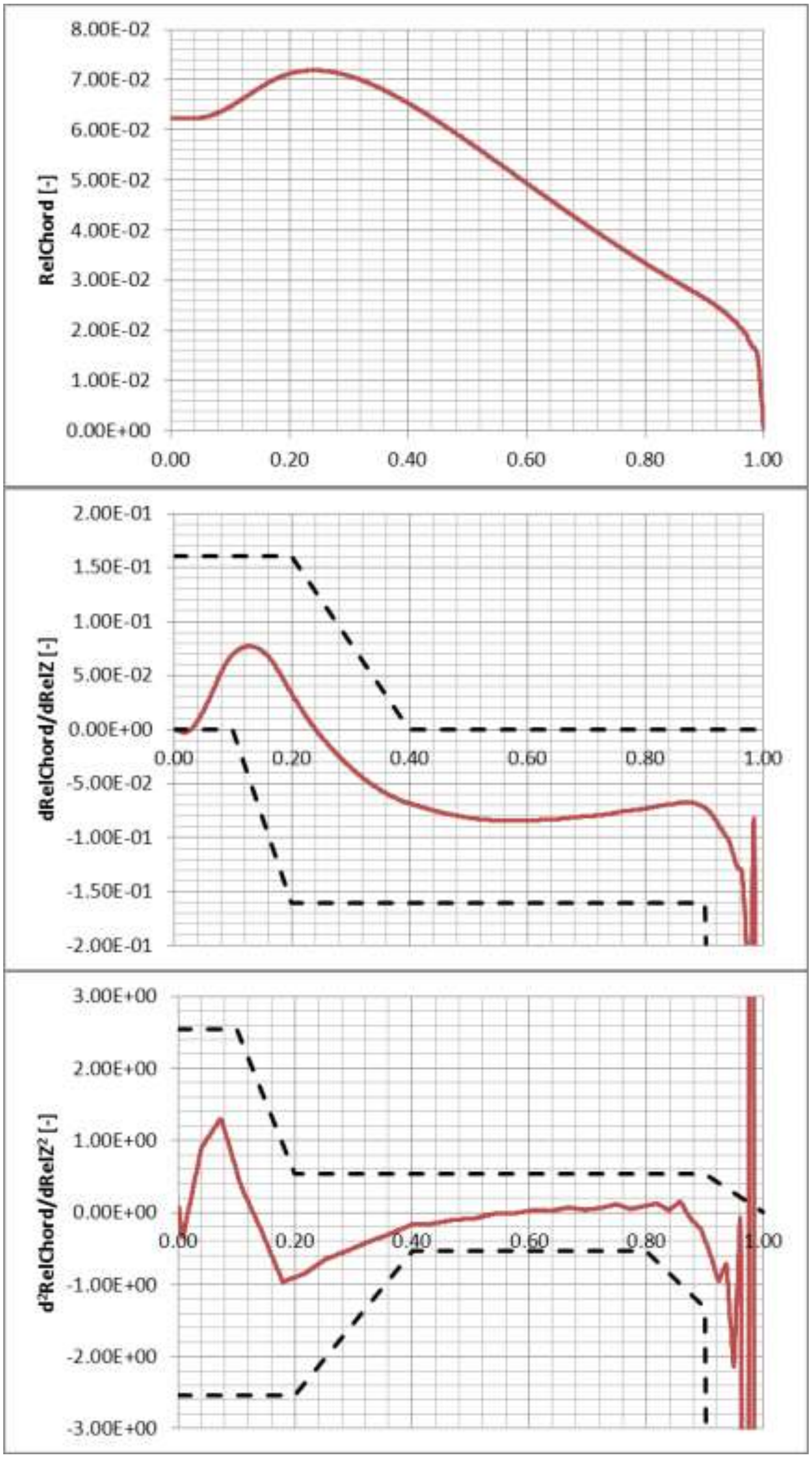

Figure 3: *RelChord*, first derivative and second derivative distributions of the INNWIND blade with AVATAR blade Min and Max values as dotted lines.

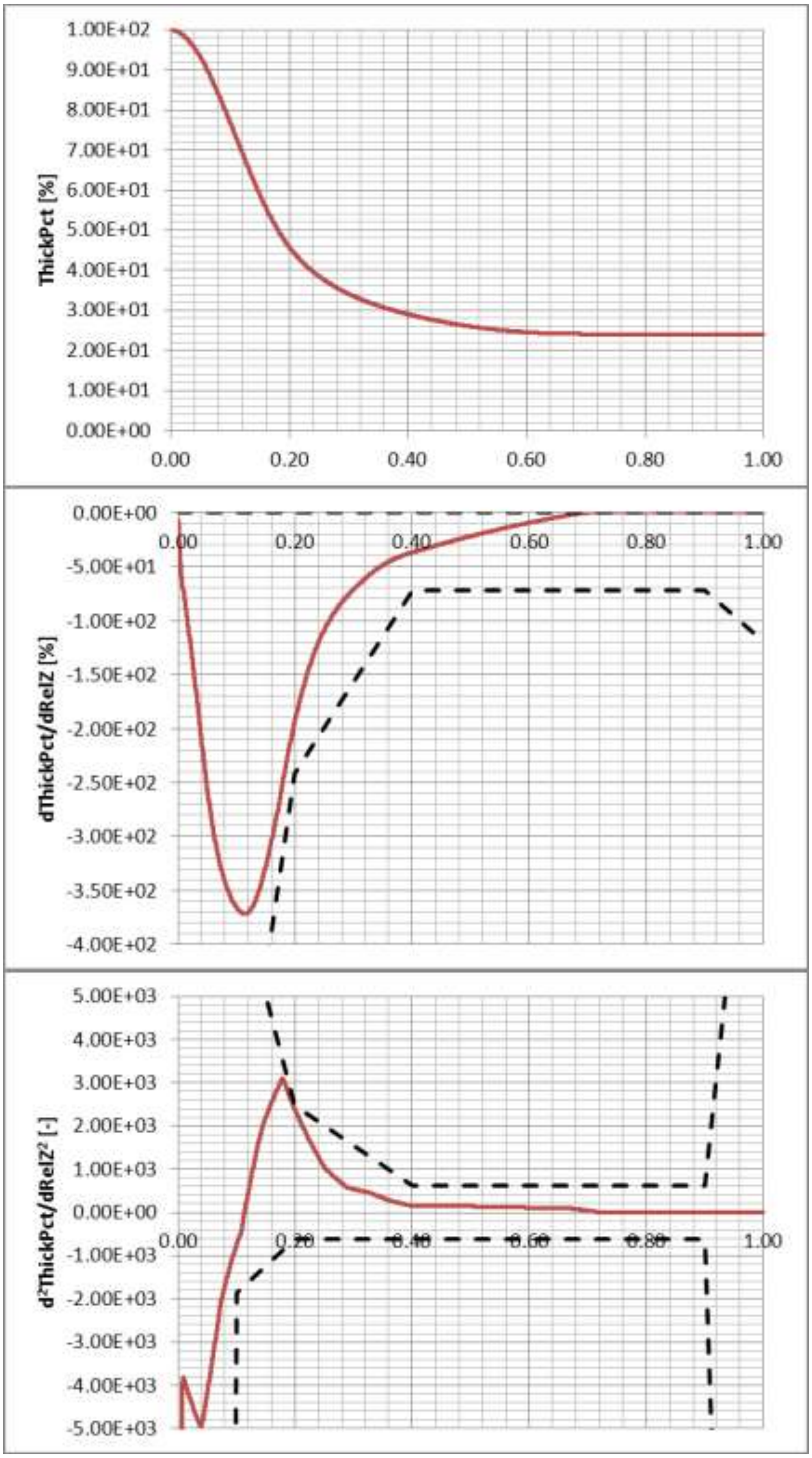

Figure 4: *ThickPct*, first derivative and second derivative distributions of the INNWIND blade with AVATAR blade Min and Max values as dotted lines.

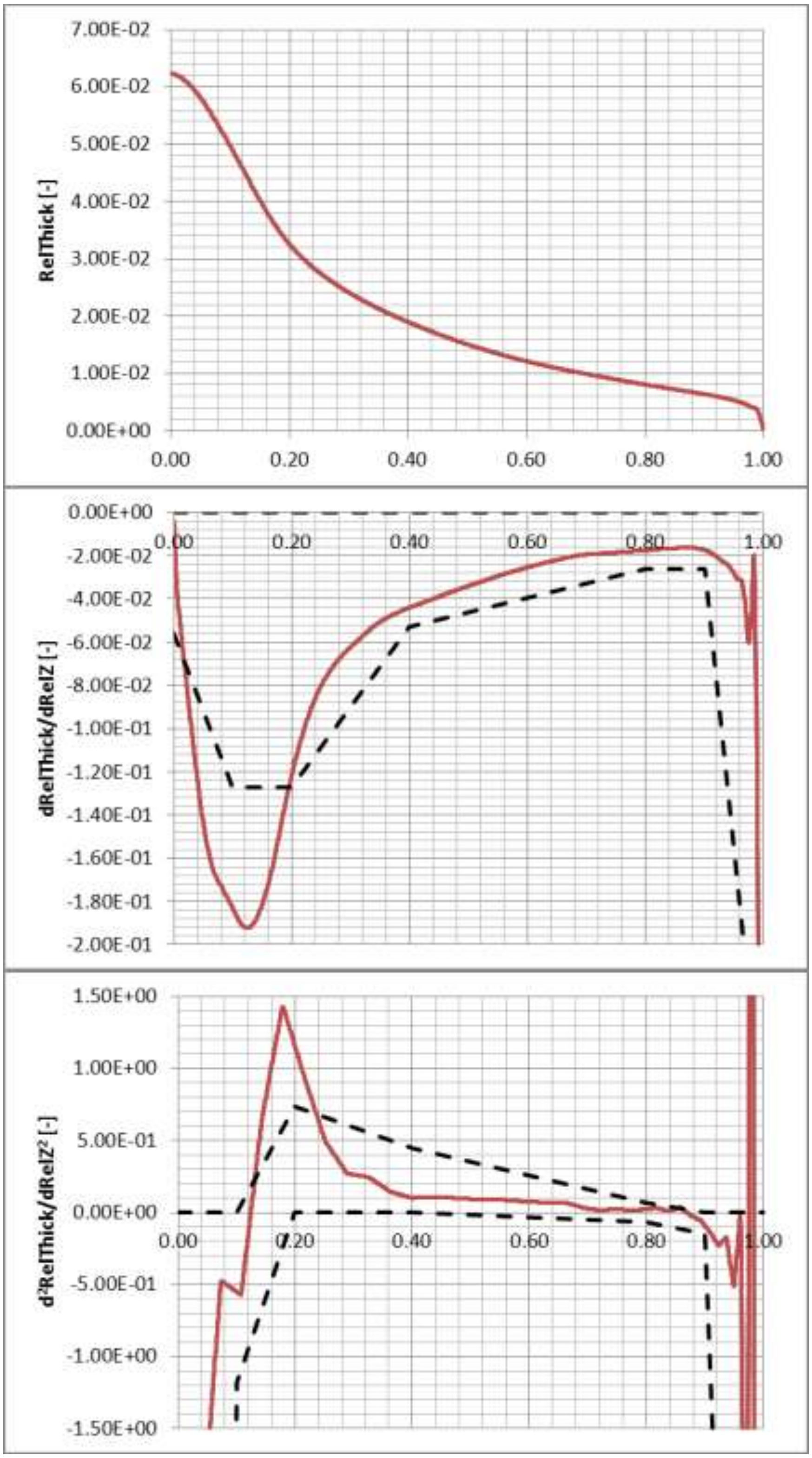

Figure 5: *RelThick*, first derivative and second derivative distributions of the INNWIND blade with AVATAR blade Min and Max values as dotted lines.

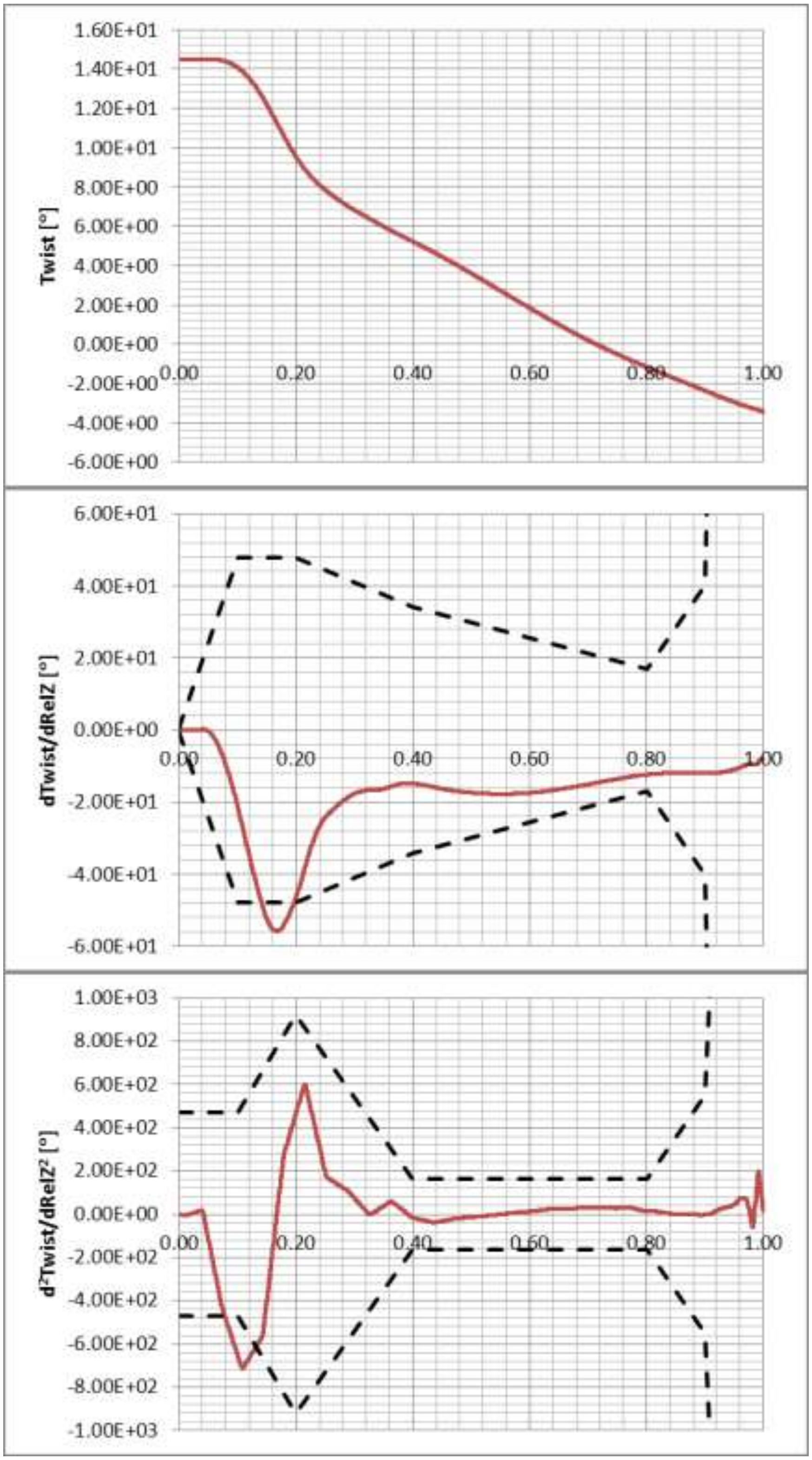

Figure 6: *Twist*, first derivative and second derivative distributions of the INNWIND blade with AVATAR blade Min and Max values as dotted lines.